

Highly Efficient Full-Vectorial Integral Equation Solution for the Bound, Leaky, and Complex Modes of Dielectric Waveguides

Svetlana V. Boriskina, *Member, IEEE*, Trevor M. Benson, *Senior Member, IEEE*, Phillip Sewell, *Member, IEEE*, and Alexander I. Nosich, *Senior Member, IEEE*

Abstract—A full-vectorial contour integral equation analysis of the natural modes of dielectric waveguides (DW) of arbitrary cross section is presented. The Galerkin method, together with the Analytical Regularization procedure, is applied to discretizing and solving the eigenvalue problem. This ensures the fast convergence and superior accuracy of the numerical algorithms. The waveguide cross section is characterized by a parametrical curve defining its contour, with a limited curvature at each point. This avoids the singularity points at corner regions and provides accurate results, even for waveguides with virtually sharp corners. Both fundamental and higher order mode propagation characteristics are studied in the bound, leaky, and complex regimes. Numerical results consistent with other theories and experimental data are presented for a wide range of practical dielectric waveguides that demonstrate the efficiency, accuracy, and versatility of the method developed. Finally, the technique is applied to model a fused fiber coupler.

Index Terms—Dielectric waveguides, Green's functions, integral equations, optical waveguide theory, vector modal methods.

I. INTRODUCTION

DIELECTRIC fibers and waveguides are essential building blocks of most optical devices and systems related to communications, sensing, and optical computing. To reduce the cost of dielectric waveguide (DW) analysis and optimization, efficient CAD simulation techniques are highly desirable. A great number of methods have been proposed for the analysis of DW natural modes, both cross-section-specific and applicable to arbitrarily shaped waveguides. They include mode matching techniques [1], effective dielectric constant approximations [2], and finite element [3], [4] and finite difference methods [5], [6]. Some of the approaches are limited to scalar, polarized, or semi-vectorial cases, while others can be applied to the full-vectorial case (see reviews [7], [8] for details).

With recent progress in computer technology, mode-solvers based on the finite difference techniques have become very popular design tools. However, except for several canonical structures, the study of arbitrary shape fibers and guides leads to problems with nonseparable boundary conditions, which

render conventional differential-operator methods ineffective. Their application, especially for the full-vectorial case, leads to large asymmetric eigenvalue problems, the numerical solution of which is not only time and memory consuming but also has unclear accuracy. The convergence of such methods is not uniformly guaranteed and actually depends on implementation. Moreover, for a full-vectorial formulation, transverse electric field components diverge at the sharp corners of DWs, making numerical methods unstable. An analytic treatment of the field behavior in the corner regions should be incorporated in the analysis [9], [10]. Thus, there is still a need for a uniformly reliable and efficient tool for modal field prediction.

An application of integral-operator formulations provides several advantages over conventional differential formulations. In this case, the radiation conditions and boundary conditions at the dielectric interfaces in a layered environment are rigorously accounted for in the formulation of the Green's function of a host medium. Furthermore, integral equation (IE) techniques are not cross-section-specific and are therefore suitable for analyzing a broad class of dielectric waveguides having arbitrary shape and refractive index profiles. Various boundary element method (BEM), finite element method (FEM), and method of moments (MoM) algorithms based on the surface and domain integral equation formulations have been proposed to study arbitrary shaped waveguides [11]–[14]. In the full-vectorial implementation, they also enable one to treat the sharp corners of DWs [14]. Domain IEs have a certain advantage as they permit treatment of waveguides of inhomogeneous cross sections, but they are strongly singular and numerical algorithms based on them are not very efficient in terms of both computation time and convergence. Therefore, contour IE techniques seem to be more promising for implementing efficient numerical techniques based on the full-vectorial problem formulation.

This paper presents a reduction of the eigenvalue problem to the contour IEs, which only requires the discretization of the contour of a DW. However, a direct application of the standard Galerkin discretization technique may present difficulties due to the singular behavior of the integral operators. A method that enables one to overcome this difficulty and obtain a stable and well-conditioned matrix equation has been proposed in [15] for two-dimensional (2-D) free-space scattering problems by dielectric cylinders. It belongs to the family of techniques collectively called method of analytical regularization [16]. In this paper, we extend the analysis to solve for the modes of regular DWs. The expansion of components in a certain set of basis

Manuscript received September 4, 2002; revised September 30, 2002. This work was supported in part by the EPSRC under Research Grant GR/R65213.

S. V. Boriskina, T. M. Benson, and P. Sewell are with the School of Electrical and Electronic Engineering, University of Nottingham, Nottingham NG7 2RD, U.K.

A. I. Nosich is with the Institute of Radio-Physics and Electronics, National Academy of Sciences of Ukraine, Kharkov 61085, Ukraine.

Digital Object Identifier 10.1109/JSTQE.2002.806729

functions and analytical inversion of the singular part of the integral operators lead to a rigorous conversion of the singular IEs to Fredholm second-kind infinite-matrix equations. This guarantees the convergence and accuracy of computations and provides a clear physical picture of various DW propagation regimes.

The guaranteed stability of the method means that we can address with confidence the higher order modes in the leaky regime for which there is a scarcity of results even for conventional circular or rectangular waveguides. It is well known that, unlike closed waveguides, for which the propagation modes are discrete and infinite in number, the spectrum of DWs is more complex. Here, there are two options. One is to impose the condition of the field decay in the cross section. Then, in addition to the discrete spectrum of proper guided natural modes, DWs are shown to support a continuous spectrum of radiation modes. The other approach is to generalize the condition at infinity in the cross section and admit the field growth. This is done by imposing the so-called Reichardt condition [17], which serves as the analytic continuation of the Sommerfeld condition to the complex domain. In this case, it is proven that the spectrum of generalized eigenwaves is discrete and located on the Riemann surface of a certain logarithmic function [17].

In most of the above-cited papers, only the bound modes were considered. The leaky modes have been quite extensively studied for striplines [18], planar dielectric guides [19] and rib waveguides [20], [21]. To date, the behavior of the circular fiber symmetrical modes in the leaky regime has been studied by using approximate analytical formulations in [22], [23], and the characteristics of its lowest HE_{1m} modes are reported in [24] but only in the weakly guiding approximation. Moreover, it has been shown that DWs can support exponentially decaying modes with complex propagation constants ("proper" complex quasieigenmodes [25]). Along with the potential applications to various optoelectronic devices, knowledge of the properties of complex, leaky, and radiation modes is essential when calculating losses due to radiation at DW discontinuities, adjacent objects, or coupling into other guiding structures. As our formulation is essentially complex, leaky and complex waves can be treated with no additional analytical or computational effort and material losses can be easily included into the analysis.

The paper is organized as follows. In Section II, the eigenvalue problem is formulated and contour integral equations are introduced. Section III details the application of the Method of Analytical Regularization to the discretization of IEs and a well-conditioned Fredholm second-kind infinite-matrix equation is obtained. Zeroes of the matrix determinant yield the propagation constants of all the natural modes of the waveguide. Numerical results are presented in Section IV for rectangular, triangular, circular, and elliptic DWs, as well as for a fused fiber coupler. Dispersion characteristics and electromagnetic field profiles in bound and leaky regimes are shown and where possible compared with published data. Finally, conclusions are given in Section V.

II. EIGENVALUE PROBLEM AND BASIC EQUATIONS

Consider the propagation of electromagnetic waves in an open isotropic uniform-cladding waveguide of arbitrary cross

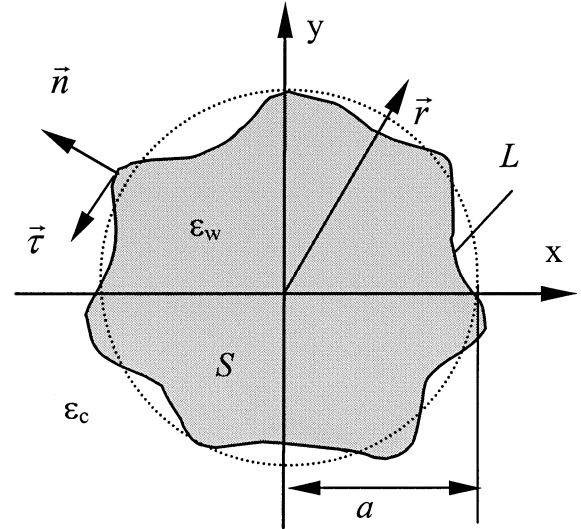


Fig. 1. Cross section of a dielectric waveguide. L is an original arbitrary smooth contour, and circle of radius a is the standard contour for which an analytical solution exists.

section, as shown in Fig. 1. The uniform core and cladding media are characterized by constant refractive indices n_w, n_c or dielectric constants ϵ_w, ϵ_c , respectively. A cross section of the DW is bounded by a closed doubly continuously differentiable curve L that can be uniquely described by the parametric expressions: $x = x(s), y = y(s), 0 \leq s \leq 2\pi$, where s is a parameterization parameter. As will be shown later in this paper, a wide class of optical guides of practical interest can be described by defining the exact form of parametric expression for L . A local rectangular coordinate system may be chosen as shown in Fig. 1 (\vec{n} and $\vec{\tau}$ are normal and tangential unit vectors to the contour L , respectively). The time dependence is assumed to be $\exp\{-i\omega t\}$ and is suppressed throughout the paper. As we consider longitudinally invariant waveguides, assume that the only z dependence for the unknowns is $\exp\{ik\beta z\}$, where β is a propagation constant in the z direction and k is the free-space wavenumber.

The total field is to satisfy the Maxwell equations with corresponding coefficients in each material and the conditions of continuity at the contour L

$$\begin{aligned} \nabla \times \vec{E} - ik\vec{H} &= 0 \\ \nabla \times \vec{H} + ik\epsilon(\vec{r})\vec{E} &= 0. \end{aligned} \quad (1)$$

Here, $\epsilon(\vec{r}) = \epsilon_w$ or ϵ_c , respectively, and

$$\begin{aligned} \vec{E} &= \vec{E}(\vec{r})e^{ik\beta z} \\ \vec{H} &= \vec{H}(\vec{r})e^{ik\beta z} \\ \vec{r} &= \{x, y\}. \end{aligned} \quad (2)$$

We shall take the basic components to be E_z and H_z and derive all the other components from them. Integration along the z axis furnishes a Fourier transform of the three-dimensional (3-D) problem and makes it 2-D. The basic field components should then satisfy a pair of coupled scalar wave equations

$$\begin{aligned} \Delta_{\perp} E_z^{w(c)} + k^2 \gamma_{w(c)}^2 E_z^{w(c)} &= 0 \\ \Delta_{\perp} H_z^{w(c)} + k^2 \gamma_{w(c)}^2 H_z^{w(c)} &= 0. \end{aligned} \quad (3)$$

The conditions of continuity of tangential components of the fields across the contour L can be written as follows:

$$\frac{1}{\gamma_w^2} \left(\beta \frac{\partial E_z^w}{\partial \tau} - \frac{\partial H_z^w}{\partial n} \right) - \frac{1}{\gamma_c^2} \left(\beta \frac{\partial E_z^c}{\partial \tau} - \frac{\partial H_z^c}{\partial n} \right) = 0 \quad (4)$$

$$\frac{1}{\gamma_w^2} \left(\beta \frac{\partial H_z^w}{\partial \tau} + \varepsilon_w \frac{\partial E_z^w}{\partial n} \right) - \frac{1}{\gamma_c^2} \left(\beta \frac{\partial H_z^c}{\partial \tau} + \varepsilon_c \frac{\partial E_z^c}{\partial n} \right) = 0 \quad (5)$$

$$E_z^w - E_z^c = 0 \quad (6)$$

$$H_z^w - H_z^c = 0 \quad (7)$$

where $\gamma_w = \sqrt{\varepsilon_w - \beta^2}$, $\gamma_c = \sqrt{\varepsilon_c - \beta^2}$, $\partial/\partial n$ is the outer normal derivative, and $\partial/\partial \tau$ is the tangential derivative to the contour L . Besides, as we consider an open-domain problem, a Reichardt condition at infinity should be imposed [17].

The fields in the core and the cladding can be presented in the form of single-layer surface potentials over the contour of the DW cross section (subscripts w and c have been omitted for compactness)

$$E_z(\vec{r}) = \int_L e(\vec{r}_s) G(\vec{r}, \vec{r}_s) dl_s, \\ H_z(\vec{r}) = \int_L h(\vec{r}_s) G(\vec{r}, \vec{r}_s) dl_s. \quad (8)$$

The kernel functions G_w , G_c are the Green's functions of the uniform media with permittivity ε_w and ε_c , respectively, and are given by the following expression:

$$G(\vec{r}, \vec{r}_s) = \frac{i}{4} H_0^{(1)}(k\gamma |\vec{r} - \vec{r}_s|). \quad (9)$$

Here, $H_0^{(1)}(\cdot)$ is the zeroth-order Hankel function of the first kind. By imposing the continuity of the unknown tangential components of the electric and magnetic fields at the core/cladding interface, we obtain the set of coupled contour IEs

$$\int_0^{2\pi} e_w(s') G_w(s, s') L(s') ds' - \int_0^{2\pi} e_c(s') G_c(s, s') L(s') ds' = 0 \quad (10)$$

$$\int_0^{2\pi} h_w(s') G_w(s, s') L(s') ds' - \int_0^{2\pi} h_c(s') G_c(s, s') L(s') ds' = 0 \quad (11)$$

$$\frac{\beta}{\gamma_w^2} \int_0^{2\pi} e_w(s') \frac{\partial G_w(s, s')}{\partial \tau} L(s') ds' - \frac{1}{\gamma_w^2} \left(\frac{h_w(s)}{2} + \int_0^{2\pi} h_w(s') \frac{\partial G_w(s, s')}{\partial n} L(s') ds' \right) - \frac{\beta}{\gamma_c^2} \int_0^{2\pi} e_c(s') \frac{\partial G_c(s, s')}{\partial \tau} L(s') ds' + \frac{1}{\gamma_c^2} \left(-\frac{h_c(s)}{2} + \int_0^{2\pi} h_c(s') \frac{\partial G_c(s, s')}{\partial n} L(s') ds' \right) = 0 \quad (12)$$

$$\frac{\beta}{\gamma_w^2} \int_0^{2\pi} h_w(s') \frac{\partial G_w(s, s')}{\partial \tau} L(s') ds' + \frac{\varepsilon_w}{\gamma_w^2} \left(\frac{e_w(s)}{2} + \int_0^{2\pi} e_w(s') \frac{\partial G_w(s, s')}{\partial n} L(s') ds' \right) - \frac{\beta}{\gamma_c^2} \int_0^{2\pi} h_c(s') \frac{\partial G_c(s, s')}{\partial \tau} L(s') ds' - \frac{\varepsilon_c}{\gamma_c^2} \left(-\frac{e_c(s)}{2} + \int_0^{2\pi} e_c(s') \frac{\partial G_c(s, s')}{\partial n} L(s') ds' \right) = 0 \quad (13)$$

where the vectors \vec{r} , \vec{r}_s refer to points along the contour L . The complex values of the parameter β for which a nontrivial solution of the set (10)–(13) exists give the propagation constants of the waveguide eigenmodes.

III. OUTLINE OF THE ANALYTICAL REGULARIZATION METHOD

According to (8), the behavior of the kernels of the IEs (10) and (11) is determined by the behavior of the Hankel functions $H_0^{(1)}(k\gamma_{w(c)}|\vec{r} - \vec{r}_s|)$. The latter are known to have logarithmic singularities at $\vec{r} \rightarrow \vec{r}_s$. The kernels of the integrals in the IEs in (12) and (13) are normal and tangential derivatives of the Green's functions on the contour of the waveguide. On the contour with a continuous curvature κ , normal derivatives of the Green's functions have finite limit values at $\vec{r} \rightarrow \vec{r}_s$, determined by the value of the contour curvature. Finally, the integral operators with the kernels represented by tangential derivatives of the Green's functions have Cauchy type singularity at $\vec{r} \rightarrow \vec{r}_s$. The presence of these singularities may present considerable difficulties for the effective solution of the integral equations. We suggest exploiting the fact that the integral operators for the circular fiber problem have the same type of kernel singularities, while the problem is known to have an analytical solution. The Green's functions and their derivatives for the case of a circular fiber of radius a can be written as follows (subscripts w and c are omitted):

$$G^0(s, s') = \frac{i}{4} H_0^{(1)} \left(2ka\gamma \left| \sin \frac{s-s'}{2} \right| \right), \quad (14)$$

$$\frac{\partial}{\partial n} G^0(s, s') = -\frac{ik\gamma}{4} \left| \sin \frac{s-s'}{2} \right| \cdot H_1^{(1)} \left(2ka\gamma \left| \sin \frac{s-s'}{2} \right| \right), \quad (15)$$

$$\frac{\partial}{\partial \tau} G^0(s, s') = -\frac{ik\gamma \sin(s-s')}{8} \left| \sin \frac{s-s'}{2} \right|^{-1} \cdot H_1^{(1)} \left(2ka\gamma \left| \sin \frac{s-s'}{2} \right| \right). \quad (16)$$

Therefore, by adding and subtracting the integral operators for the circular case to the (10)–(13), we can perform an analytical regularization of the singular IEs (10)–(13). Using the functions $\{e^{imt}\}_{m=-\infty}^{\infty}$, which are the orthogonal eigenfunctions of all the integral operators (14)–(16), as a global basis in the Galerkin discretization scheme we combine the analytical regularization and discretization of integral equations. Thus, expanding the kernel functions and unknown field densities in (10)–(13) in terms of the Fourier series and performing

term-by-term integration and differentiation, we obtain an infinite set of matrix equations

$$e_m^w H_m^w J_m^w - e_m^c H_m^c J_m^c + \sum_{n=-\infty}^{\infty} A_{mn}^w e_n^w - \sum_{n=-\infty}^{\infty} A_{mn}^c e_n^c = 0 \quad (17)$$

$$h_m^w H_m^w J_m^w - h_m^c H_m^c J_m^c + \sum_{n=-\infty}^{\infty} A_{mn}^w h_n^w - \sum_{n=-\infty}^{\infty} A_{mn}^c h_n^c = 0 \quad (18)$$

$$\begin{aligned} & \frac{i\beta m}{\gamma_w^2} e_m^w H_m^w J_m^w - \frac{i\beta m}{\gamma_c^2} e_m^c H_m^c J_m^c \\ & - \frac{\beta}{\gamma_w} \sum_{n=-\infty}^{\infty} B_{mn}^w e_n^w + \frac{\beta}{\gamma_c} \sum_{n=-\infty}^{\infty} B_{mn}^c e_n^c \\ & - \frac{ka}{\gamma_w} h_m^w H_m^w J_m^w + \frac{ka}{\gamma_c} h_m^c H_m^c J_m^c \\ & - \frac{1}{\gamma_w} \sum_{n=-\infty}^{\infty} C_{mn}^w h_n^w + \frac{1}{\gamma_c} \sum_{n=-\infty}^{\infty} C_{mn}^c h_n^c = 0 \end{aligned} \quad (19)$$

$$\begin{aligned} & \frac{ka\varepsilon_w}{\gamma_w} e_m^w H_m^w J_m^w - \frac{ka\varepsilon_c}{\gamma_c} e_m^c H_m^c J_m^c \\ & + \frac{\varepsilon_w}{\gamma_w} \sum_{n=-\infty}^{\infty} C_{mn}^w e_n^w - \frac{\varepsilon_c}{\gamma_c} \sum_{n=-\infty}^{\infty} C_{mn}^c e_n^c \\ & + \frac{i\beta m}{\gamma_w^2} h_m^w H_m^w J_m^w - \frac{i\beta m}{\gamma_c^2} h_m^c H_m^c J_m^c \\ & - \frac{\beta}{\gamma_w} \sum_{n=-\infty}^{\infty} B_{mn}^w h_n^w + \frac{\beta}{\gamma_c} \sum_{n=-\infty}^{\infty} B_{mn}^c h_n^c = 0 \end{aligned} \quad (20)$$

where

$$A_{mn}^{w(c)} = \frac{1}{4\pi^2} \int_0^{2\pi} \int_0^{2\pi} A^{w(c)}(s, s') e^{-ims} e^{ins'} ds ds' \quad (21)$$

and $J_m^{w(c)} = J_m(ka\gamma_{w(c)})$, $H_m^{w(c)} = H_m^{(1)}(ka\gamma_{w(c)})$ are the Bessel and Hankel functions, respectively, and the prime represents the derivative with respect to the argument. Coefficients $B_{mn}^{w(c)}$ and $C_{mn}^{w(c)}$ are defined similar to (21). Here all the functions expanded into the double Fourier series are constructed as the differences between the original IE kernels and the kernels for the circular case and thus are regular at $s = s'$. They and their limit values at $s \rightarrow s'$ are as follows (subscripts w and c are omitted):

$$A(s, s') = H_0^{(1)}(k\gamma R) - H_0^{(1)}\left(2ka\gamma \left|\sin \frac{s-s'}{2}\right|\right),$$

$$\lim_{s \rightarrow s'} A(s, s') = \frac{2i}{\pi} \ln \frac{L(s')}{a} \quad (22)$$

$$B(s, s') = K_\tau(s, s') \frac{H_1^{(1)}(k\gamma R)}{kR} - ka \frac{\sin(s-s')}{2} \left|\sin \frac{s-s'}{2}\right|^{-1} \cdot H_1^{(1)}\left(2ka\gamma \left|\sin \frac{s-s'}{2}\right|\right),$$

$$\lim_{s \rightarrow s'} B(s, s') = 0 \quad (23)$$

$$C(s, s') = K_n(s, s') \frac{H_1^{(1)}(k\gamma R)}{kR} + ka \left|\sin \frac{s-s'}{2}\right| \cdot H_1^{(1)}\left(2ka\gamma \left|\sin \frac{s-s'}{2}\right|\right),$$

$$\lim_{s \rightarrow s'} C(s, s') = \frac{2}{i\pi\gamma} (\kappa(s') L(s') - 1) \quad (24)$$

$$K_n(s, s') = k^2 \left(x'(s) (y(s) - y_s(s')) - y'(s) (x(s) - x_s(s')) \right)$$

$$K_\tau(s, s') = k^2 \left(x'(s) (x(s) - x_s(s')) + y'(s) (y(s) - y_s(s')) \right) \quad (25)$$

where $R = \sqrt{(x - x_s)^2 + (y - y_s)^2}$. Note that all the matrix elements $A_{mn}^{w(c)}$, $B_{mn}^{w(c)}$, and $C_{mn}^{w(c)}$ turn to zero in the case of a circular contour L . Following [15], one can verify that the matrix operators A, B , and C are compact in the space l_2 if the contour L is a smooth curve without sharp edges. The homogeneous block-matrix (17)–(20) will only have nontrivial solutions for discrete values of the longitudinal propagation constant β corresponding to the zeros of the matrix determinant. Once the zeros of the determinantal equation are found, the electric and magnetic field profiles can be calculated.

In open structures like optical waveguides, the propagation eigenproblem, consisting of the Helmholtz equation together with the boundary conditions at the core/cladding interface and Reichardt condition at infinity, is not self-adjoint. As a consequence, modes having complex-valued propagation constants can exist even in the DWs with no material losses. These are leaky modes that grow at infinity, whose eigenvalues are located on the second, nonphysical sheet of the Riemann surface of the function $\ln \gamma_c(\beta) = \ln \sqrt{\varepsilon_c - \beta^2}$, and “proper” complex modes that have fields vanishing at infinity in the waveguide cross section with eigenvalues located on the physical sheet of the Riemann surface [25]. Both characterize physical field oscillations and are not spurious solutions that arise due to the numerical method used for computations. Therefore, the search for zeros of the determinant has to be performed in the complex plane rather than on the real axis.

Due to the Fredholm second-kind nature of (17)–(20), a uniform accuracy of the numerical algorithm can be achieved provided that the truncated matrix size N is adapted to the waveguide parameters. It also results in small matrices, thus reducing the computation time. Fig. 2 shows the computation error as a function of the truncated matrix size. It can clearly be seen that the smoother the contour of the DW cross section then the smaller the final matrix size. Furthermore, larger values of the truncation number should be taken to calculate higher order modes with the same degree of accuracy as principal modes. For example, it is sufficient to take $N = 7$ and $N = 23$ to achieve a guaranteed accuracy of the propagation constants of the principal modes of the elliptical and rectangular waveguides considered in Section IV, respectively, up to the fourth decimal place in the sensitive normalized propagation constant. CPU time per iteration, including filling the matrix and root finding, was 3

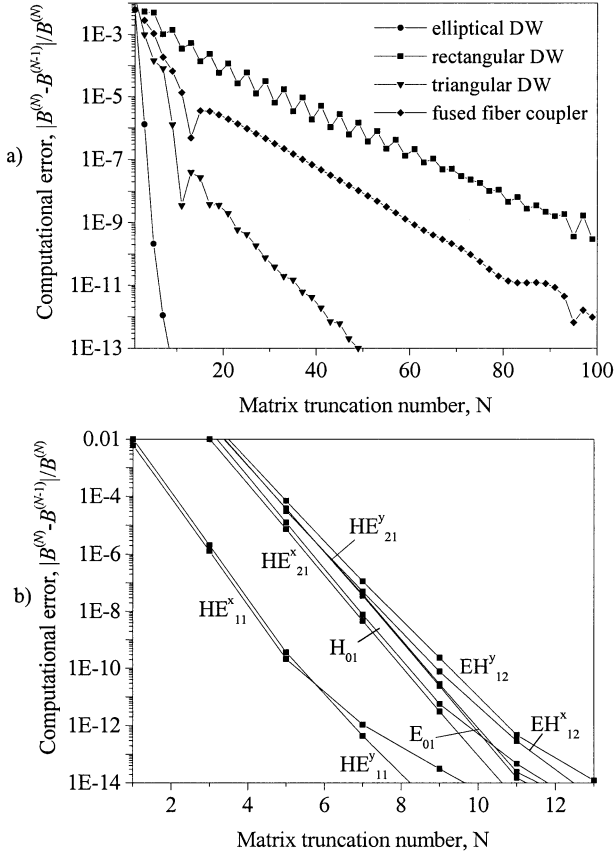


Fig. 2. Computational errors of the normalized propagation constants: (a) principal modes of DWs of various shapes and (b) principal and higher order modes of the elliptical waveguide.

s for the elliptical and 8 s for the rectangular waveguide on a 999-MHz PC.

IV. SIMULATIONS OF OPTICAL WAVEGUIDES

In this section we demonstrate the performance of the method developed by studying a number of examples. The refractive index profile of the core of a general step-index dielectric waveguide is characterized by the refractive index step: $\Delta n = (n_w - n_c)/n_w$. It should be noted that unlike vectorial finite-difference mode solvers the present method does not have any numerical drawback for high-index-contrast waveguides. The modal dispersion characteristics are the dependences of the normalized propagation constant B , on the normalized frequency V , where

$$B = \frac{\beta^2 - \varepsilon_c}{\varepsilon_w - \varepsilon_c}, \quad (26)$$

$$V = \frac{kb}{\pi} \sqrt{\varepsilon_w - \varepsilon_c}$$

where b is a characteristic size of the DW minor axis.

A. Buried Rectangular Dielectric Waveguide

As a first example, we consider a buried rectangular-core waveguide. The rectangular cross section is described by using the “super-ellipse” formula [15]

$$\begin{aligned} x &= b\mu \cos s \cdot r(s) \\ y &= b\sin s \cdot r(s) \\ r(s) &= (|\cos s|^{2\nu} + |\sin s|^{2\nu})^{-1/2\nu}. \end{aligned} \quad (27)$$

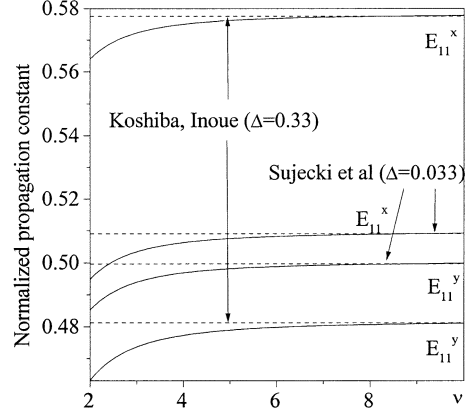


Fig. 3. Normalized propagation constants versus superellipse parameter ν .

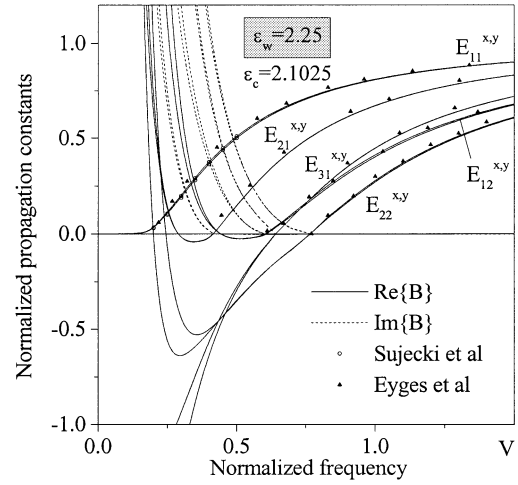


Fig. 4. Dispersion characteristics of a rectangular DW ($n_w = 1.5$, $n_c = 1.45$, $\mu = 2$, and $\nu = 10$).

The greater the value of parameter ν , the closer the shape of the cross section approaches that of a rectangle (the case of $\nu = 1$ corresponds to the elliptical cross section). First, to validate such an approximation of the contour, we study the change of the normalized propagation constant B with the increasing parameter ν . The results are presented in Fig. 3 for two cases: high ($\Delta n = 0.33$) and low ($\Delta n = 0.033$) index steps. The reference data have been taken from [6] and [13], respectively, for the waveguides with parameters: $n_w = 1.5$, $n_c = 1.45$, $\mu = 2$ and $n_w = 1.5$, $n_c = 1.0$, $\mu = 2$. It can be seen that in both cases it is enough to take a value of ν equal to 10 or greater to get a sufficient approximation of a rectangle.

The modal dispersion characteristics of the rectangular-core waveguide are shown in Fig. 4. For comparison, the numerical data of a vectorial finite-difference method [6] (circles) and scalar contour integral equation technique [11] (triangles) are depicted for the bound modes. In this figure, as well as all the following ones, the solid and dashed curves correspond to the real and imaginary parts of the normalized modal propagation constants, respectively. It can be seen that the principal $E_{11}^{x,y}$ modes are proper surface waves having a purely real B for any value of the frequency, while other modes become leaky ones below the cutoff frequencies. Rigorous study of the mode coupling requires considering the whole spectrum of the DW

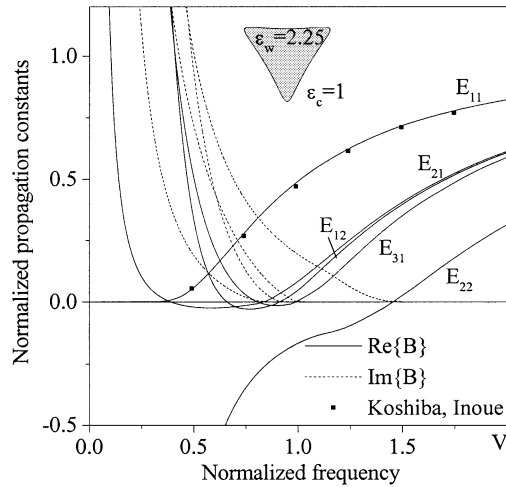


Fig. 5. Dispersion characteristics of an equilateral triangular waveguide. ($n_w = 1.5$, $n_c = 1.0$).

modes. Knowing the modal properties of the leaky modes is of great importance since waveguide discontinuities, such as bends, junctions, and shape imperfections, cause the excitation of the radiation and leaky modes.

B. Equilateral Curvilinear Triangular DW

Next, we consider another geometry with virtually sharp corners, an equilateral triangular core waveguide. A parametric expression for a smooth approximation of a triangular contour can be written as follows:

$$\begin{aligned} x &= b \left(\sin s - \sin \frac{2s}{3} \right) \\ y &= -b \left(\cos s + \cos \frac{2s}{3} \right). \end{aligned} \quad (28)$$

Fig. 5 shows the dispersion characteristics of the triangular-core DW. The results for the fundamental E_{11}^y mode are consistent with those obtained in [3] using FEM and BEM. As the figure shows, all the hybrid modes are degenerate. This is because of the symmetry of the structure, e.g., the odd mode about the line $\varphi = 60^\circ$ is, in fact, a superposition of two even modes about $\varphi = 120^\circ$ and $\varphi = 270^\circ$ and vice versa, so that their propagation constants are identical. The explanation of this feature of the triangular-core waveguide has been given in [26]. However, due to the round-off errors, the point-matching technique applied in [26] was unable to successfully show the degeneracy.

C. Dielectric Waveguides of Circular and Elliptic Cross Sections: Optical Fibers

Next, the modal analysis of circular and elliptical fibers, shown in the insets of Figs. 6 and 7, is performed. The modal dispersion characteristics for the first seven modes of a circular fiber are presented in Fig. 6. These results coincide with the exact solutions of the well-known transcendental eigenvalue equation for circular fibers. Due to the spatial symmetry of the fiber cross section, all the natural modes apart from E_{0n} and H_{0n} are double-degenerate.

Elliptical waveguides enable one to remove the mode polarization degeneracy and therefore provide stability of the mode patterns against DW shape imperfections or environmental

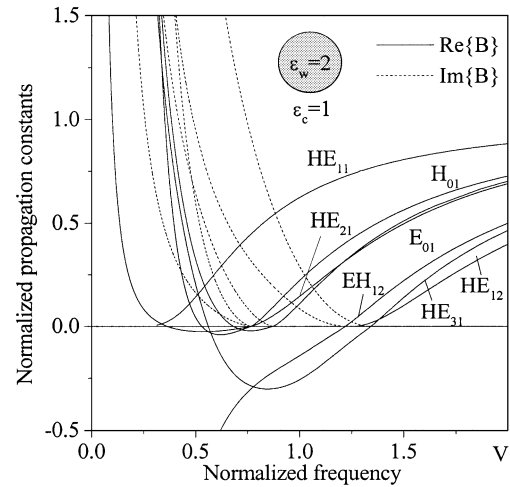


Fig. 6. Dispersion characteristics of a circular fiber ($n_w = 1.41$, $n_c = 1.0$).

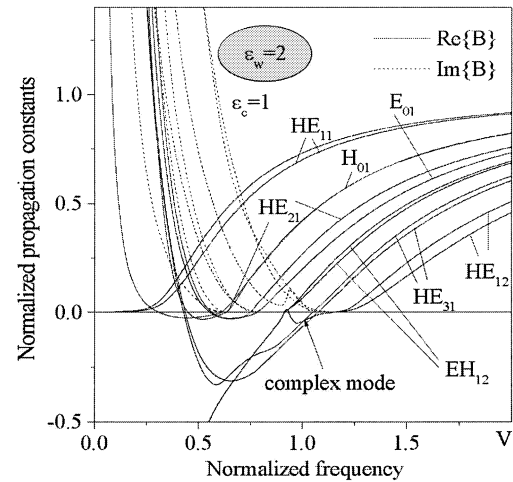


Fig. 7. Dispersion characteristics of the elliptical waveguide ($n_w = 1.41$, $n_c = 1.0$, $\mu = 1.5$).

changes. Thus, polarization-maintaining elliptical DWs find applications in dual-mode fiber-optics systems and coherent optical transmission [4]. Fig. 7 presents the modal dispersion characteristics of an elliptic DW. It can be clearly seen that all the double-degenerate modes split into two polarizations, the value of the polarization birefringence being different for various modes. The polarization birefringence depends strongly on the core ellipticity and increases with an increase in the elongation parameter μ .

The mode intensity profiles in bound, complex and leaky regimes are shown in Fig. 8(a)–(c), respectively. As can be seen from Fig. 7, when reaching the cut-off frequency, the hybrid mode HE_{12} becomes first a complex mode and, as the parameter V decreases, a classical leaky mode.

D. Fused Fiber Couplers

Finally, to demonstrate the versatility of the contour IE method, two geometries of a fused fiber coupler depicted in the insets of Fig. 9(a) and (b) are considered. The coupler essentially consists of two optical fibers brought into close proximity in order to transfer the power from one channel to another or split or combine the power of different channels. Here, the

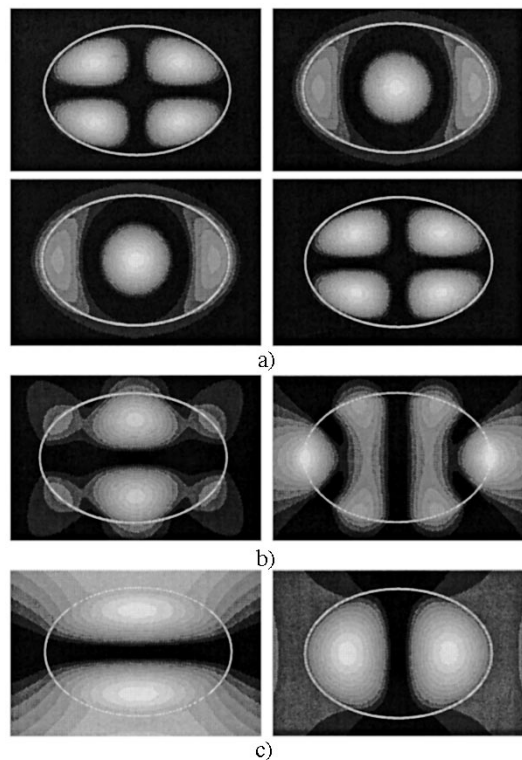


Fig. 8. Transformation of the HE_{12} hybrid mode of the elliptic fiber ($n_w = 1.41$, $n_c = 1.0$, and $\mu = 1.5$): E_z and H_z field profiles of (a) bound modes, (b) complex modes, and (c) leaky modes.

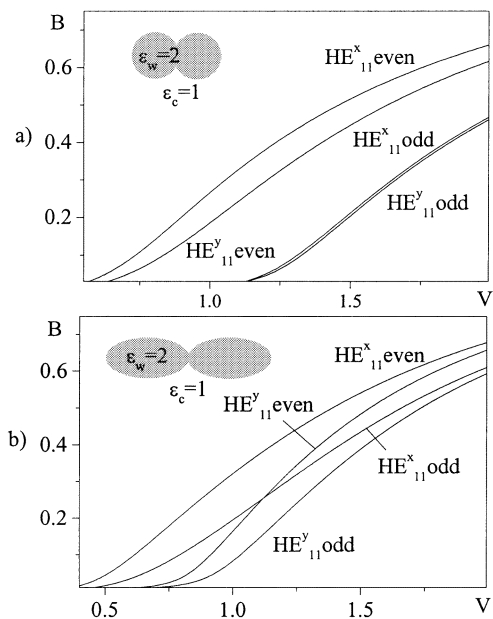


Fig. 9. Dispersion characteristics of the fused fiber couplers. (a) $n_w = 1.41$, $n_c = 1.0$, $\mu = 0.81$, and $\delta = 0.4$. (b) $n_w = 1.41$, $n_c = 1.0$, $\mu = 1.5$, and $\delta = 0.49$.

coupling occurs between two pairs of modes, $HE_{11}^{x,y}$ even/odd, for odd and even field distributions, respectively. A parametric expression for a fused fiber coupler can be written as follows:

$$x = b\mu \cos s \cdot r(s), \quad y = b \sin s \cdot r(s), \quad r(s) = \delta(1 - \cos 2s) + 1. \quad (29)$$

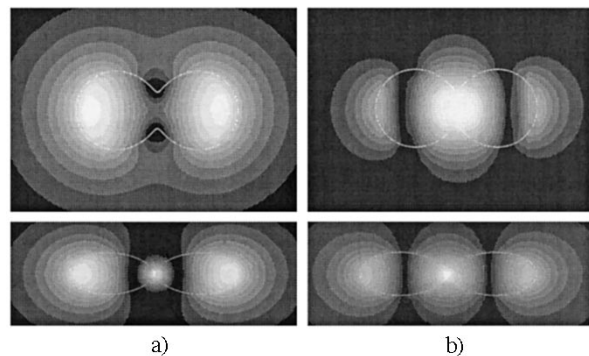


Fig. 10. Field intensity profiles of (a) HE_{11}^x even and (b) HE_{11}^x odd modes of the fused fiber couplers with the same parameters as in Fig. 9.

The dispersion characteristics of the four principal modes of the circular and elliptical fiber coupler are plotted in Fig. 9. The field distributions of HE_{11}^x even and odd modes of both couplers are shown in Fig. 10.

V. CONCLUSION

A full-vectorial analysis using contour integral equation formulation for the study of natural modes of dielectric waveguides has been presented. A set of contour IEs has been obtained from a rigorous integral representation of the fields and further discretized by using a global-basis Galerkin method together with the Analytical Regularization technique. This results in a final block-matrix equation of the Fredholm second kind, which guarantees the stability and a very fast convergence of the numerical algorithm as well as reduction of the computer time and memory resources. Sample results have been presented for several practical geometries. To establish the validity of the present method, we demonstrated a very good agreement with the propagation constants of bound modes obtained by other methods for some conventional waveguide structures. Furthermore, we investigated the properties of the leaky and complex modes of the same waveguides. Finally, the characteristics of the fused optical fiber coupler were studied.

The method can be used for the study of the polarization-dependent properties of a wide range of waveguide-based photonic structures. One of the attractive features of the approach proposed is that it is formulated in the complex domain and so immediately allows calculation of leaky modes and the treatment of lossy and amplifying media. The method is very versatile and with some modifications may be applied to waveguides of arbitrary geometrical shapes located in the layered dielectric media, such as rib waveguides of various profiles, multicladding fibers, and dielectric image guides.

ACKNOWLEDGMENT

The authors wish to thank Prof. P. Kendall, University of Nottingham, U.K., and Dr. Y. Karchevskii, Kazan State University, Russia, for useful discussions and critical advice.

REFERENCES

- [1] E. Yamashita, K. Atsuki, O. Hashimoto, and K. Kamijo, "Modal analysis of homogeneous optical fibers with deformed boundaries," *IEEE Trans. Microwave Theory Tech.*, vol. MTT-27, pp. 352–256, Apr. 1979.

- [2] K. S. Chiang, C. H. Kwan, and K. M. Lo, "Effective-index method with built-in-perturbation correction for the vector modes of rectangular-core optical waveguides," *J. Lightwave Technol.*, vol. 17, pp. 716–722, Apr. 1999.
- [3] M. Koshiba and K. Inoue, "Simple and efficient finite-element analysis of microwave and optical waveguides," *IEEE Trans. Microwave Theory Techn.*, vol. 40, pp. 371–377, Feb. 1992.
- [4] M. Eguchi and M. Koshiba, "Accurate finite-element analysis of dual-mode highly elliptical-core fibers," *J. Lightwave Technol.*, vol. 12, pp. 607–613, Apr. 1994.
- [5] C. L. Xu, W.-P. Huang, M. Stern, and S. K. Chaundhuri, "Full-vectorial mode calculations by finite difference method," *Proc. Inst. Elec. Eng.—Optoelectron.*, vol. 141, pp. 281–286, May 1994.
- [6] S. Sujecki, T. M. Benson, P. Sewell, and P. C. Kendall, "Novel vectorial analysis of optical waveguides," *J. Lightwave Technol.*, vol. 16, pp. 1329–1335, July 1998.
- [7] S. M. Saad, "Review of numerical methods for the analysis of arbitrary-shaped microwave and optical dielectric waveguides," *IEEE Trans. Microwave Theory Techn.*, vol. 33, pp. 894–899, Oct. 1985.
- [8] C. Vassallo, "1993–1995 optical mode solvers," *Opt. Quantum Electron.*, vol. 29, pp. 95–114, 1997.
- [9] W. W. Lui, C.-L. Xu, W.-P. Huang, K. Yokoyama, and S. Seki, "Full-vectorial mode analysis with considerations of field singularities at corners of optical waveguides," *J. Lightwave Technol.*, vol. 17, pp. 1509–1513, Aug. 1999.
- [10] Y.-P. Chiou, Y.-C. Chiang, and H.-C. Chang, "Improved three-point formulas considering the interface conditions in the finite-difference analysis of step-index optical devices," *J. Lightwave Technol.*, vol. 18, pp. 243–251, 2000.
- [11] L. Eyges, P. Gianino, and P. Wintersteiner, "Modes of dielectric waveguide of arbitrary cross sectional shape," *J. Opt. Soc. Amer.*, vol. 69, pp. 226–235, 1979.
- [12] C. D. Nallo, F. Frezza, and A. Galli, "Full-wave modal analysis of arbitrary-shaped dielectric waveguides through an efficient boundary-element method formulation," *IEEE Trans. Microwave Theory Techn.*, vol. 43, pp. 2982–2990, Dec. 1995.
- [13] J. Bagby, D. Nyquist, and B. C. Drachman, "Integral formulation for analysis of integrated dielectric waveguides," *IEEE Trans. Microwave Theory Techn.*, vol. 33, pp. 906–915, Oct. 1985.
- [14] D.-U Li and H.-C. Chang, "An efficient full-vectorial finite-element modal analysis of dielectric waveguides incorporating inhomogeneous elements across dielectric discontinuities," *IEEE J. Quantum Electron.*, vol. 36, pp. 1251–1261, Nov. 2000.
- [15] A. I. Nosich and S. V. Boriskina, "Economical and accurate in resonances solution to the scattering by arbitrary dielectric cylinders based on the canonical-shape inversion," *IEEE Trans. Antennas Propagat.*, 2001, submitted for publication.
- [16] A. I. Nosich, "MAR in the wave-scattering and eigenvalue problems: Foundations and review of solutions," *IEEE Antennas Propagat. Mag.*, vol. 41, pp. 34–49, Mar. 1999.
- [17] Y. M. Karchevskii, A. I. Nosich, and G. W. Hanson, "Mathematical analysis of the generalized natural modes of an inhomogeneous optical fiber," *Math. Meth. Appl. Sci.*, 2002, submitted for publication.
- [18] L. O. McMillan, N. V. Shuley, and P. W. Davis, "Leaky fields on microstrip," *Progr. Electromagn. Res.*, vol. PIER 17, pp. 323–337, 1997.
- [19] S. Yamaguchi, A. Shimojima, and T. Hosono, "Analysis of leaky modes supported by a slab waveguide," *Electron. Commun. Japan*, pt. 2, vol. 73, no. 11, pp. 9–18, 1990.
- [20] H. E. Hernández-Figueroa, F. A. Fernández, Y. Lu, and J. B. Davies, "Vectorial finite element modeling of 2D leaky waveguides," *IEEE Trans. Magnetics*, vol. 31, pp. 1710–1713, May 1995.
- [21] S. S. A. Obayya, B. M. A. Rahman, K. T. V. Grattan, and H. A. El-Mikati, "Full vectorial finite-element-based imaginary distance beam propagation solution of complex modes in optical waveguides," *J. Lightwave Technol.*, vol. 20, pp. 1054–1060, June 2002.
- [22] R. A. Sammut and A. W. Snyder, "Leaky modes of circular optical waveguides," *Appl. Opt.*, vol. 15, pp. 477–482, February 1976.
- [23] V. V. Shevchenko, "About the behavior of the dielectric waveguide wavenumbers below cutoff (media with material losses)," *Izvestiya Vysshih Uchebnyh Zavedenii, Radiofizika*, vol. 15, pp. 59–67, 1972.
- [24] L. A. Melnikov and E. A. Romanova, "Behavior of HE_{1m} mode wavenumbers of optical fiber below the cutoff frequency," *Opt. Commun.*, vol. 116, pp. 358–364, May 1995.
- [25] T. F. Jablonski, "Complex modes in open lossless dielectric waveguides," *J. Opt. Soc. Amer. A*, vol. 11, pp. 1272–1282, Apr. 1994.
- [26] J. R. James and I. N. L. Gallett, "Modal analysis of triangular-cored glass-fiber waveguide," *Proc. Inst. Elect. Eng.*, vol. 120, pp. 1362–1369, Nov. 1973.

Svetlana V. Boriskina (S'96–M'00) was born in Kharkov, Ukraine, in 1973. She received the M.Sc. degree in radio physics (with honors) and the Ph.D. degree from Kharkov National University, Kharkov, Ukraine, in 1995 and 1999, respectively.

From 1997 to 1999, she was a Researcher in the School of Radio Physics at Kharkov National University and, in 2000, a Royal Society—NATO Post-Doctoral Fellow in the School of Electrical and Electronic Engineering, University of Nottingham, Nottingham, U.K. Currently, she works there as a Research Associate. Her research interests are in integral equation methods for electromagnetic wave scattering and eigenvalue problems in layered media, with applications to microwave and optical waveguides, dielectric resonators, and antennas.

Trevor M. Benson (M'95–SM'01) was born in Sheffield, U.K., in 1958. He received the First Class honors degree in physics and the Ph.D. degree in electronic and electrical engineering from the University of Sheffield, Sheffield, U.K., in 1979 and 1982, respectively.

After spending over six years as a Lecturer at University College Cardiff, he joined the University of Nottingham as a Senior Lecturer in Electrical and Electronic Engineering in 1989. He was promoted to the posts of Reader in Photonics in 1994 and Professor of Optoelectronics in 1996. His present research interests include experimental and numerical studies of electromagnetic fields and waves, with particular emphasis on propagation in optical waveguides and lasers, silicon-based photonic circuits, and electromagnetic compatibility.

Prof. Benson received the Clark Prize in Experimental Physics from the University of Sheffield.

Phillip Sewell (S'88–M'91) was born in London, U.K., in 1965. He received the B.Sc. degree in electrical and electronic engineering (with first class honors) and the Ph.D. degree from the University of Bath, Bath, U.K., in 1988 and 1991, respectively.

From 1991 to 1993, he was an S.E.R.C. Post-Doctoral Fellow at the University of Ancona, Italy. Since 1993, he has been a Lecturer and from 2001, a Reader in the School of Electrical and Electronic Engineering at the University of Nottingham, Nottingham, U.K. His research interests involve analytical and numerical modeling of electromagnetic problems, with application to optoelectronics, microwaves, and electrical machines.

Alexander I. Nosich (M'94–SM'95) was born in Kharkov, Ukraine, in 1953. He graduated from the School of Radio Physics of the Kharkov National University, Kharkov, Ukraine, in 1975 and received the Ph.D. and D.Sc. degrees in radio physics from the same university in 1979 and 1990, respectively.

Since 1978, he has been on the research staff of the Institute of Radio-Physics and Electronics (IRE) of the Ukrainian Academy of Sciences, Kharkov. In 1992–2002, he held research fellowships and visiting professorships in Turkey, Japan, France, and Italy. Currently, he is a leading scientist in the Department of Computational Electromagnetics, IRE. His research interests include methods of analytical regularization, free-space and open-waveguide scattering, complex mode behavior, radar cross-section analysis, and antenna simulation.